Materials and Interfaces

Scilight

Communication

Check for updates

Effect of Electropolishing on Morphology and Adhesion of Nanostructured Anodic Tantalum Oxide Thin Films

Sarah E. Pooley [1], Cyrus Koroni [1], Shinthia Binte Eskender [1], Jacob Olson [1], Joshua A. Russell [1], Max Bork [1], Timothy Merrell [1], Gage Cook [1], Scarlet Fields [1], Kaden Kunz [1], Kiev Dixon [1], Pete Barnes [2], Brian Jaques [1], and Hui Xiong [1,*]

[1] Micron School of Materials Science and Engineering, Boise State University, Boise, ID 83720, USA
[2] Idaho National Laboratory, Idaho Falls, ID 83415, USA
* Correspondence: clairexiong@boisestate.edu

Received: 17 July 2026; Revised: 13 August 2026; Accepted: 24 August 2026; Published: 3 September 2026

Abstract: Anodic tantalum oxide films have attracted significant interest due to their highly favorable properties, such as corrosion resistance and biocompatibility, as well as the cost-effective and scalable nature of anodization as a fabrication method. However, the need for morphological control as well as strong adhesion of the resulting films to the substrate pose barriers to their application. In this work, the morphology and adhesion of anodic tantalum oxide films grown on electropolished, chemically etched, and pristine tantalum metal substrates in a fluoride-free electrolyte containing potassium phosphate and glycerol under varying voltage and temperature conditions were systematically investigated. Electropolishing significantly reduced substrate surface roughness and promoted the growth of native suboxide species. Current density-time characteristics during anodization suggest noticeable kinetic effects related to substrate pre-preparation, which were corroborated by significantly increased pore size in oxide films grown on electropolished substrates. Systematic variation in voltage and temperature provided evidence of improved control over size and morphology of the nanoporous anodized oxide films via anodization parameters in electropolished samples. In addition, pull tests demonstrated increased film-substrate adhesion in anodized oxide films on both chemically etched and electropolished substrates. These findings demonstrate that electropolishing is an effective strategy for improving the controllability of nanostructure morphology, film uniformity, and adhesion of anodic tantalum oxide coatings.

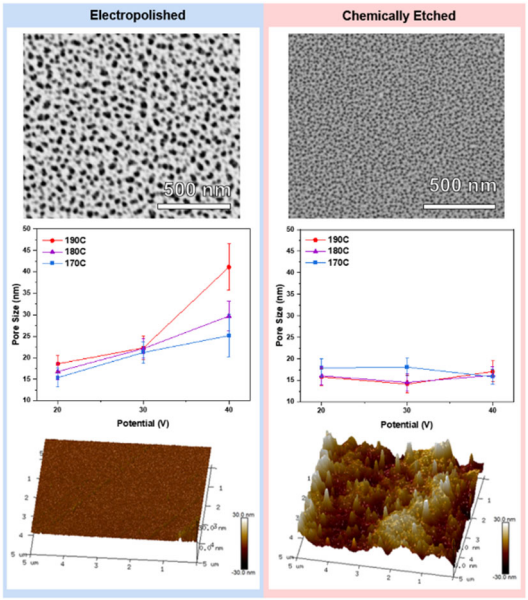

Keywords: electropolishing; anodization; morphology; adhesion; tantalum oxide

1. Introduction

Tantalum oxide has attracted considerable interest for use in a variety of technologically significant applications, including catalysts [1], information storage devices [2–5], and protective coatings for biomedical applications [6]. Across these diverse fields, nanostructure plays a key role by affecting material properties such as photocatalytic activity [1], hydrophilicity [7], and memristive behavior [8]. In particular, nanoporous and nanotubular oxide films have been demonstrated to improve lithium ion diffusion kinetics for energy storage applications [9], as well as increase photocatalytic efficiency of water splitting for hydrogen generation [10]. For biomedical and photoelectrochemical applications, film structure and adhesion are especially critical, as they directly affect implant biocompatibility [6] and catalyst performance [11,12]. Consequently, strategies that enable precise control over oxide nanostructure and adhesion are of significant interest.

Electrochemical anodization utilizes competing field-assisted oxide formation and dissolution reactions during electrochemical oxidation of a valve metal substrate to grow nanostructured anodic oxide layers of controlled thickness and porosity [13,14]. It is notably cost-effective and scalable among the synthesis methods used for forming oxide coatings, particularly for Ta_2O_5. In order to facilitate the formation of highly ordered and well-adhered nanostructures, electropolishing is a popular substrate preparation technique prior to anodic oxide growth, as it enables efficient polishing to nanoscale smoothness [15,16]. The two techniques have previously been used in tandem to improve uniformity of oxide films grown via anodization such as Al_2O_3 [17,18], TiO_2 [19], and Nb_2O_5 [16]. However, limited work has been done in understanding the effect of electropolishing on the anodization of tantalum [6,20–22].

The wide variety of electrolyte systems and conditions which have been investigated for tantalum anodization have been comprehensively summarized in recent review articles [23,24]. Fluoride-containing solutions predominate in prior work concerning nanostructured films [23], and the effect of fluoride concentration on oxide growth rate [25] and porosity [26] has been investigated in detail. However, several studies have indicated that the incorporation of fluoride ions into the anodic tantalum oxide films is a major factor responsible for film detachment and poor substrate adhesion [23,27–29], as a result of the enhanced inward mobility of fluoride ions compared to oxygen [30] and the subsequent build up of fluoride containing species between the oxide layer and the substrate [28]. Consequently, the use of non-fluoride-containing electrolyte solutions serves as an alternative to improve film adhesion, which is critical for a wide range of applications [23] including photoelectrochemical [11] and biomedical [6] purposes. Melody et al. first reported the anodization of tantalum foil using 10% dibasic potassium phosphate in glycerol at elevated temperatures (90–190 °C) and anodizing potential of 20 V [13]. Later, Lee and Schmuki investigated the effect of temperature and time on pore ordering and film thickness in the same electrolyte system, identifying a 1-h anodization procedure at 20 V and 180 °C as the conditions for optimal pore ordering. The formation of a 25 nm barrier layer at the anodic oxide-substrate interface was identified, but its effect on film adhesion was not studied [31]. By improving overall homogeneity of the substrate via electropolishing as well as removing the highly soluble fluoride-based barrier layer, strong attachment of the anodic oxide to the substrate may be facilitated.

Here, we report a systematic study on the effect of electropolishing of Ta substrates on the morphology and adhesion of anodic Ta_2O_5 films grown in 10% potassium phosphate in glycerol electrolyte. The influence of anodization potential, electrolyte temperature, and the presence of the native suboxide species on the substrate were investigated. Atomic force microscopy (AFM) and x-ray photoelectron spectroscopy (XPS) were utilized to examine the roughness and surface chemistry of electropolished, chemically etched, and pristine tantalum foils. Current density transients during anodization were obtained to investigate the effect of native suboxide species on the anodization process. The morphology and thickness of the resulting anodic oxide films was examined using scanning electron microscopy (SEM). In addition, pull tests were used to investigate film adhesion. We demonstrate that while both chemical etching and electropolishing improve film-substrate adhesion compared to pristine samples, electropolishing offers more control over pore size and morphology of the resulting anodic oxide films, by facilitating the continuous competition between oxide growth & dissolution fundamental to nanostructure formation.

2. Materials and Methods

2.1. Substrate Preparation

Pieces of tantalum foil (33 × 40 × 0.127 mm, 99.95% purity, Thermo Fisher Scientific, Waltham, MA, USA) were cleaned by sonication in acetone, isopropanol, and deionized water, for five minutes each, and dried prior to substrate preparation. The back of each piece was masked using packing tape, with the top edge of the foil left exposed to ensure good electrical contact in the case of electropolishing. Chemically etched samples were allowed to soak in a solution of 10% sulfuric acid in methanol for at least one hour before being rinsed in deionized water and dried immediately prior to anodization. Electropolishing was performed in a two-electrode cell with Ta foil as both the working and counter electrode using a solution of 10% sulfuric acid in methanol (Thermo Fisher Scientific, Waltham, MA, USA), prepared as previously described by Barnes et al. [16]. During electropolishing, the solution was kept below −10 °C in a bath of dry ice and acetone and continuously stirred. Samples were electropolished at a constant current of 0.1 A for 2 h using a BK 9206 power supply (B&K Precision Corporation, Yorba Linda, CA, USA). Following polishing, the foils were removed from solution, rinsed in deionized water, dried, and immediately placed under vacuum and transferred into an inert atmosphere glovebox (Ar, O_2 <0.5 ppm).

2.2. Anodization

Total air exposure for both chemically etched and electropolished substrates prior to anodization was kept to less than 10 min. Kapton tape was used to mask the back of all samples prior to anodization. Exposed working electrode area was 33 × 40 mm. Anodization was performed in a two-electrode cell using 10% dibasic potassium phosphate (98% pure, Thermo Fisher Scientific, Waltham, MA, USA) in glycerol (Thermo Fisher Scientific, Waltham, MA, USA) with Pt mesh as the counter electrode. Anodization was carried out under constant voltage with a current limit of 2 A. Anodization time was fixed at 5 min, while solution temperature (170–190 °C) and applied potential (20–40 V) conditions were systematically varied. Following anodization, samples were rinsed in deionized water and ethanol before being allowed to dry.

2.3. Characterization

The surface roughness of pristine, chemically etched, and electropolished samples was characterized using a Bruker Dimension Icon atomic force microscope (AFM) with a Nanoscope V controller operated in PeakForce Tapping Mode by Nanoscope 9.4 software using a ScanAsyst Air probe (2 nm nominal tip radius). 5 × 5 μm images were taken with a scan rate of 0.5 Hz, 256 samples per line, and Peak Force setpoint of 2 nN. AFM images were processed using Nano Scope Analysis (Bruker Nano, Santa Barbara, CA, USA). Scanning electron microscopy (SEM) images were recorded using an FEI Teneo FESEM (Field Electron and Ion Company, Hillsboro, OR, USA) at 3–5 kV. X-ray photoelectron spectroscopy (XPS) was performed using a Physical Electronics (PHI) 5600 ESCA system (Physical Electronics, Chanhassen, MN, USA) with a monochromated Al K-alpha source and 3 × 10 mm analysis area. Survey scans were performed using 187.85 eV pass energy and 0.8 eV step size; high resolution scans were performed using 23.50 eV pass energy and 0.05 eV step size. XPS data was analyzed using MultiPak 9.6 (Physical Electronics, Chanhassen, MN, USA) and CasaXPS (Casa Software Ltd., casaxps.com; accessed 26 August 2026). All spectra were referenced to the 1s peak (284.8 eV) of adventitious carbon. Spectra were background subtracted and subsequently deconvoluted using the standard FWHM positions for each of the known valence states. Fit constraints included constant binding energy separation and area ratios of 1.91 eV and 4:3 respectively. Adhesion tests were performed in accordance with ASTM standard D4541-22 using a DeFelsko AT-A20 A-B adhesion tester (DeFelsko, Ogdensburg, NY, USA). ResinLab EP11HT 2-Part Epoxy (ResinLab, Germantown, WI, USA) was used to adhere 10 mm Al dollies to the anodic oxide coating prior to pull tests, where the coating was exposed to 7550 N of pressure for 129.1 s at a rate of 60 N/s with 5 s hold. Measurements were duplicated for each sample grown on pristine, chemically etched, and electropolished substrates.

3. Results and Discussion

3.1. Effect of Substrate Preparation on Oxide Morphology

Ta foil substrates were prepared under three conditions prior to anodization: (1) pristine foil, which was degreased via sonication in acetone, isopropyl alcohol, and deionized water for 5 min each prior to use; (2) chemically etched foil, which was degreased and then soaked in a solution of 10% sulfuric acid (H_2SO_4) in methanol for at least 60 min prior to use; and (3) electropolished foils, which were prepared based upon a method adapted from Barnes et al. [16] and Piotrowski et al. [15]. The effects of pretreatment on substrate morphology were characterized using AFM and are shown in Figure 1a–c. Surface roughness increased following chemical etching (R_q = 10.6 nm) compared to the pristine sample (R_q = 8.54 nm). For the electropolished sample, roughness decreased by approximately 3.81 nm (R_q = 4.73 nm) and surface homogeneity significantly improved. AFM measurements were conducted on duplicates for the electropolished condition, with <0.36 nm standard deviation in R_q.

Tantalum metal is known to have native oxide and suboxide species present on the surface, which have been theorized to be responsible for its notable corrosion resistance and biocompatibility [32]. Consequently, one of the reasons for the use of hydrofluoric acid (HF) in the majority of anodization solutions used in the literature is the need for chemicals capable of etching through the native passivation layer. In order to investigate the effect of surface preparation on the native suboxide, samples were prepared and immediately transferred to an Ar-atmosphere glovebox, where an air-free vessel was used to enable chemical characterization with XPS (Figure 1d–f); for the electropolished condition, measurements on duplicates were performed in order to check for differential charging and verify reproducibility. All XPS spectra were calibrated to the position of the 1s peak of adventitious carbon (284.8 eV) prior to deconvolution and fitting. For the electropolished sample, the Ta^{5+} 4f peak doublet appears at 26.74 eV ($4f_{7/2}$) and 28.64 eV ($4f_{5/2}$). These values are very close to those previously reported in the literature (26.8 ± 0.2 and 28.6 ± 0.2) [33,34]. Interestingly, the 4f peak doublet is shifted in both the pristine and chemically etched foils, located at 25.79 eV & 27.74 eV and 25.99 eV & 27.89 eV, respectively. Previous work

by Chakraborti et al. ascribes the peak shift towards lower binding energies as indicative of the presence of non-stoichiometric oxides of tantalum [35], an observation which has been further corroborated by other researchers [36,37]. This implies that electropolishing may facilitate the formation of more stoichiometric native oxides, a phenomenon which may be related to the improvement in surface homogeneity. Analysis of the oxygen spectra for the same set of samples (Figure S1, Supplementary Information**)** revealed that the O1s peak for both the chemically etched and electropolished samples appears at 531.9 eV and 532.2 eV respectively, which is consistent with pentavalent tantalum oxide [35]. For the pristine sample, two distinct peaks can be observed, located at 530.1 eV and 532.0 eV. One possible explanation for this phenomenon may be the presence of lower oxidation states of tantalum within the native oxide present on the surface [35].

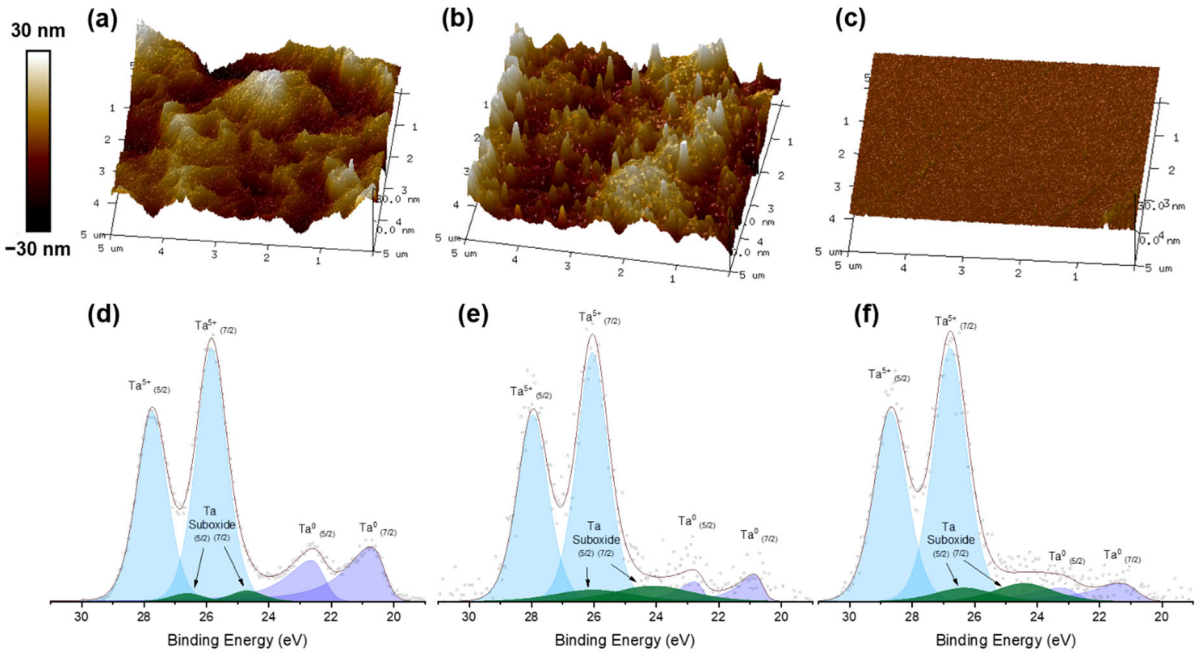

Figure 1. Topographic AFM images of (**a**) pristine, (**b**) chemically etched, and (**c**) electropolished Ta foil; Ta 4f XPS spectra of (**d**) pristine, (**e**) chemically etched, and (**f**) electropolished samples. Solid lines represent fitted curves and open dots are the experimental data.

With regard to the signal from the metal substrate, the Ta^0 peak doublet is most prominent in the spectra for the pristine sample before becoming substantially decreased following both chemical etching and electropolishing. The intensity of the suboxide peaks (24.66 eV & 26.59 eV) follows an inverse trend, increasing significantly following both substrate preparation techniques and nearly surpassing the signal from the metal substrate in the electropolished sample spectra. Quantitative oxidation-state fractions for tantalum oxide, metal, and suboxide are reported in Table S1 (Supplementary Information). These results indicate that the surface treatment of tantalum foil by chemical etching or electropolishing, even in cases involving very limited exposure to air following treatment, facilitates the growth of native suboxides.

In order to study the practical effects of surface roughness and native suboxide prevalence, anodization studies were performed for 5 min at 20 V 180 °C and a fixed current of 2 A, to allow for direct comparison of the effects of chemical and electrochemical treatment compared to the pristine foil. The current density-time ($j - t$) curves recorded during anodization are shown in Figure 2. The initial current density is between 0.111 and 0.099 A/cm^2 for all three samples, with the pristine and chemically etched samples having the highest and lowest values, respectively. Variations in duration of the current density decay reflect similar trends: for the pristine sample, its current density shows the most precipitous drop within the first minute before levelling out to a plateau until the end of the anodization period. The chemically etched sample exhibits the greatest level of decay, dropping below 0.001 A/cm^2 at just over three minutes. The electropolished sample retains higher overall current density compared to the chemically etched sample, but the curve decays continuously throughout the entire five minute period, as opposed to levelling out into the plateau characteristic of the continuous-growth behavior described by Melody et al. [13] and observed for the pristine foil within this study. One explanation for this behavior may be the increase in native suboxide prevalence following substrate preparation, which would consequently increase overall resistance at the interface and slow the electrochemical anodization process.

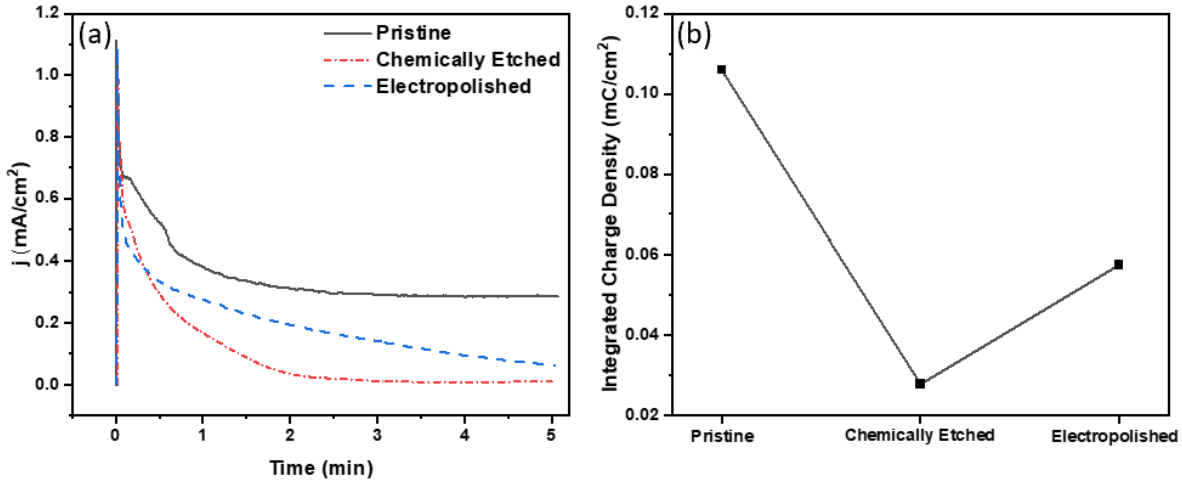

Figure 2. (**a**) Current density-time curves and (**b**) integrated charge density for anodization of pristine, chemically etched, and electropolished substrates at 20 V 180 °C.

With regard to the difference between the chemically etched and electropolished samples, namely the improved current density following electropolishing despite the increase in suboxide as indicated by XPS—the competing dissolution-growth reactions characteristic of anodization may shed some light on this phenomenon.

Nanostructuring during anodization depends upon the balance between field-assisted oxide dissolution vs. growth [14,38]. Upon formation of an initial oxide layer, field-aided ion transport of O^{2-} and Ta^{5+} ions controls further growth [38]. By continued exposure of the growing oxide to an electric field, the Ta-O bond is weakened by polarization, resulting in field-assisted metal cation dissolution, in addition to chemical dissolution by the electrolyte [39]. As a result of the interaction between these processes, suppression of oxide growth is one approach for promoting a relative increase in oxide dissolution. The shallower decay curve exhibited by the electropolished sample is consistent with continuous competition between oxide growth and dissolution, as opposed to the distinct stages seen in the pristine and chemically etched samples for continuous oxide growth. Consequently, the continuous dissolution of the oxide during relatively slow oxide growth may manifest increased current density at the electropolished surface by decreasing oxide thickness and subsequent resistance, compared to the increased resistance produced by faster oxide growth on the chemically etched surface. In order to further elucidate the effect of electropolishing and chemical etching on the balance between oxide growth and dissolution, the morphology of the anodized oxide layers, as well as their thickness and porosity, were characterized using SEM (Figure 3a–c). All three samples exhibited nanoporous morphologies with pore diameters ranging from 10 to 17 nm and an average pore size of 14.35 nm ± 0.366 nm. Interestingly, cross-sectional SEM of a total of six samples revealed substantial differences in oxide film thickness as a function of surface preparation (Figure 3d–f), providing further evidence that substrate pretreatment significantly influences anodization kinetics. The oxide film grown on the pristine substrate reached a thickness of approximately 1.43 μm, whereas the chemically etched and electropolished substrates produced progressively thinner films of approximately 0.928 μm and 0.405 μm, respectively. In addition to the reduction in thickness, the chemically etched and electropolished samples exhibited more uniform oxide layers throughout the film cross section. Several possible explanations for this phenomenon exist, such as changes in surface composition as a consequence of pre-preparation, and changes in local electric fields and surface wettability with surface roughness. Furthermore, native oxide thickness may also play a role by influencing reaction rate, as well as resistance at the electrode-electrolyte interface. With regard to the experimental results of this work, the thicker oxide formed on the pristine substrate is consistent with the XPS results, which showed a lower abundance of native suboxide species prior to anodization. A thinner native suboxide barrier facilitates ionic transport during the early stages of anodization, leading to more rapid field-assisted oxide growth and ultimately a thicker anodic film. In contrast, the higher abundance of native suboxide species on the chemically etched and electropolished substrates may increase the initial resistance to ion transport, slowing anodic oxide growth and resulting in thinner films. Notably, the electropolished substrate produced the thinnest anodic oxide layer despite exhibiting enhanced pore uniformity and nanostructural control. Combined with the current density transients, this observation suggests that electropolishing shifts the anodization mechanism toward a dynamic balance between field-assisted anodic oxide growth and oxide dissolution. In comparison, anodization of the chemically etched substrate appears to remain predominantly growth-controlled during the plateau region, resulting in greater film thickness. These findings indicate that electropolishing may modify the substrate surface

properties in a manner that promotes a more balanced anodization process, leading to improved control over anodic oxide morphology while limiting overall film growth.

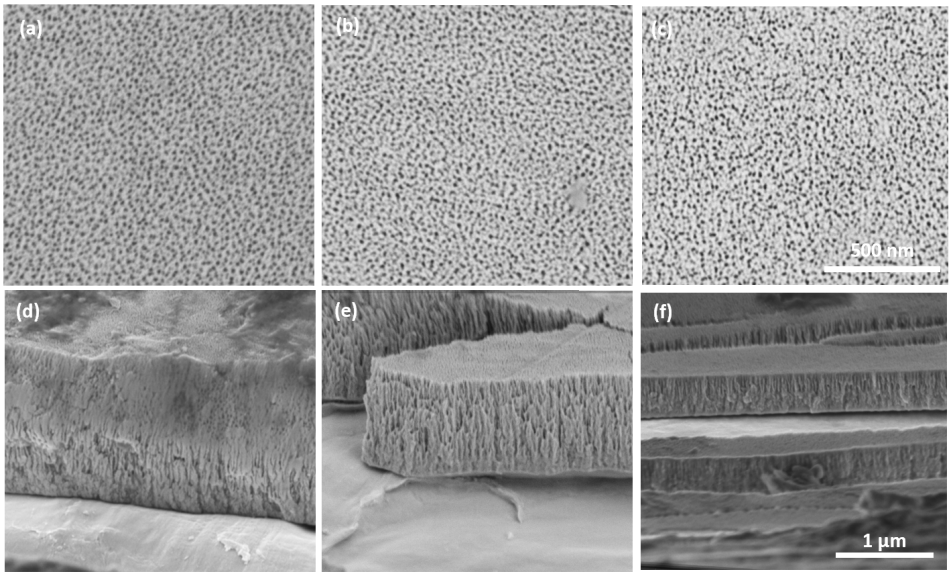

Figure 3. SEM of the top-view surface and cross-section of anodic tantalum oxide films grown at 20 V 180 °C on (**a**,**d**) pristine, (**b**,**e**) chemically etched, and (**c**,**f**) electropolished Ta foil.

3.2. Effect of Anodization Voltage and Temperature

The nanostructure of anodized films plays a key role in coating properties such as hydrophilicity [40] and diffusion kinetics [41]. During anodization, the relative rate of oxide growth versus dissolution is key to control over the size and morphology of produced nanostructures. The most typical method of increasing the rate of dissolution is via the use of stronger chemical etchants like HF, or higher applied potentials which facilitate field-assisted dissolution in addition to chemical etching. An alternative strategy is to suppress the oxide growth rate while maintaining a relatively constant dissolution rate. In the previous section, we demonstrate that substrate surface preparation modifies the abundance of native suboxide species, as well as influences anodic oxide growth kinetics without directly altering the electrolyte chemistry or anodization conditions. Next, we will investigate how anodization conditions influence the morphology of the anodized films.

To investigate how substrate pretreatment influences the morphology of the anodic oxide films in relation to anodization conditions, tantalum substrates with pristine, chemically etched, and electropolished surfaces were anodized over a range of applied voltages (20–40 V) and electrolyte temperatures (170–190 °C). Overall, electropolished substrates produced significantly larger nanopores (15–41 nm) compared to chemically etched (14–18 nm) substrates (Figure 4; Table S2, Supplementary Information). Only minor differences were observed between anodic oxide samples grown on chemically etched versus pristine substrates (Figure 3a–f). For each condition, 2–3 samples were synthesized for analysis. Pore morphology and uniformity remained relatively consistent across all conditions and substrates, with some merging of pores present in samples with increased pore sizes. More importantly, electropolished substrates exhibited a clear relationship between pore size and anodization conditions. Specifically, pore diameter exhibited a distinct increase with applied voltage (Figure 5a and Table S2), indicating that electropolishing enhances the responsiveness of pore formation to the role of the applied voltage in facilitating oxide dissolution. These observations are consistent with previous studies of tantalum anodization in fluoride-containing electrolytes. Almeida Alvez et al. [30] reported a strong linear relationship between pore size and applied voltage (20–50 V) for anodization in H_2SO_4 with HF electrolytes at room temperature, in agreement with earlier work by El-Sayed et al. [42] and more recent reviews by Mohapatra and Sulka [23]. In contrast, chemically etched samples showed no discernible correlation between pore size and anodization voltage over the same range (Figure 5b and Table S2).

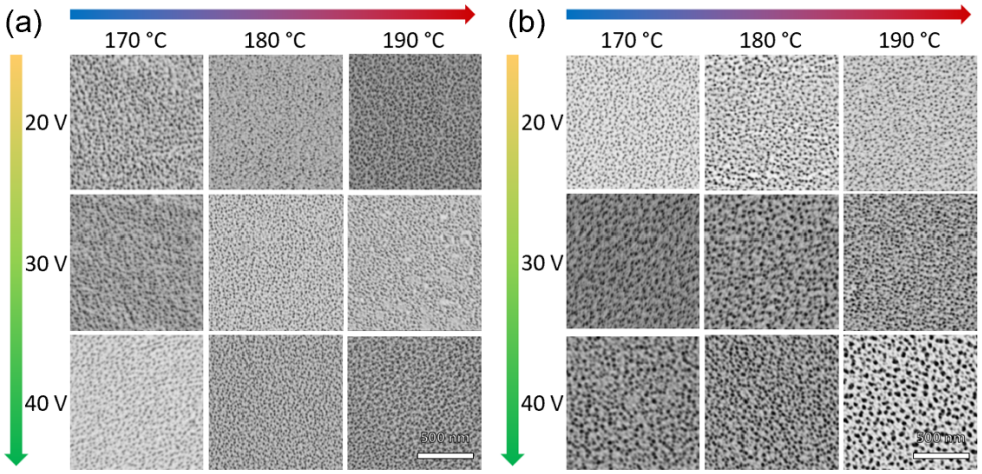

Figure 4. Top view SEM images of anodic oxide films grown at a range of voltage (20–40 V) and temperature (170–190°) conditions on (**a**) chemically etched and (**b**) electropolished substrates.

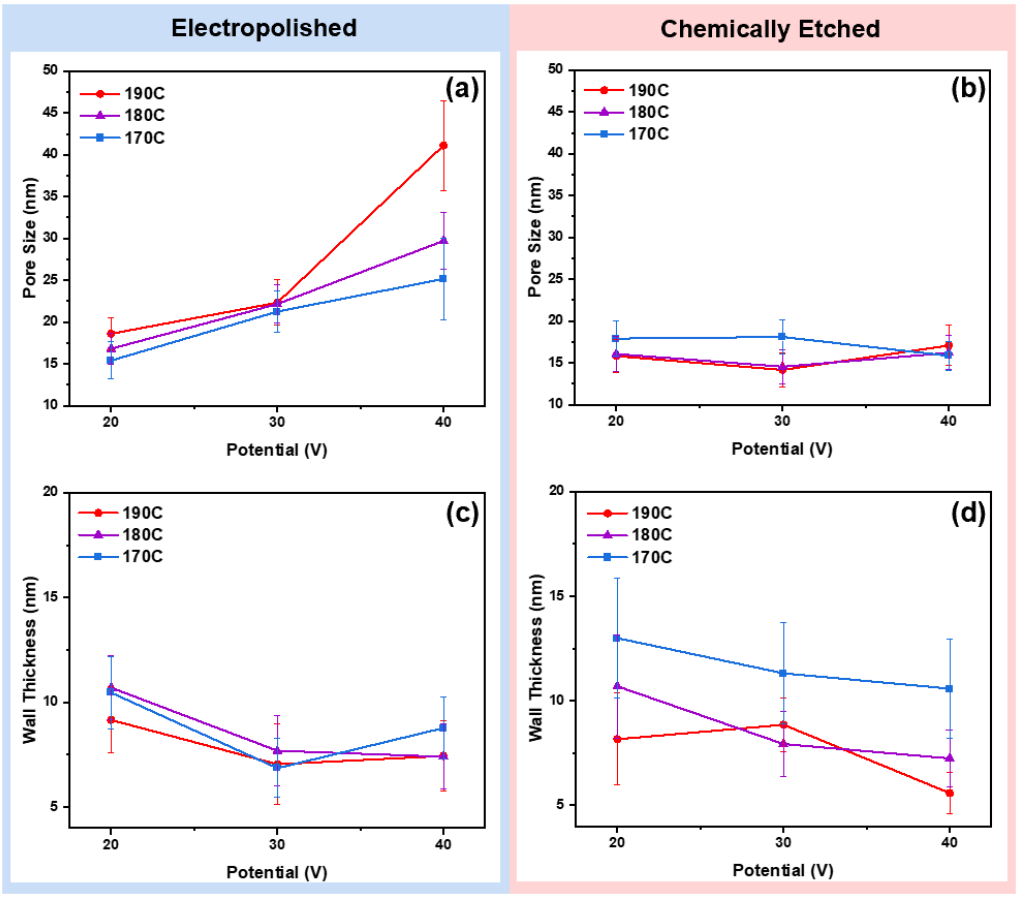

Figure 5. Trends in pore size (**a**,**b**) and wall thickness (**c**,**d**) as a function of anodization parameters for anodic tantalum oxide films grown on electropolished vs. chemically etched substrates. Error bars represent standard deviation in pore size measurements.

A similar trend was observed with electrolyte solution temperature. Increasing the solution temperature led to an average 7.53 nm increase in pore size with each 10 °C interval for electropolished substrates (Figure 5a), while the chemically etched samples remained largely insensitive to temperature. Wall thickness exhibited similar behavior between the two surface preparations (Figure 5c,d). Electropolished samples showed smaller distribution of wall thicknesses across all conditions (6.9–10.5 nm) as well as decreased standard deviation in wall thickness measurements (Table S2, Supplementary Information), while chemically etched samples displayed substantially greater variability (5.6–13.0 nm) as well as higher standard deviation (Figure 5d; Table S2, Supplementary

Information). For both substrate types, a weak dependence of wall thickness on temperature was observed, consistent with enhanced ionic diffusion and accelerated oxide dissolution at elevated temperatures.

Overall, the anodic oxide films grown on chemically etched substrates exhibited limited sensitivity to changes in anodization voltage and temperature, whereas electropolished substrates showed systematic and predictable variations in pore morphology. We hypothesize that this enhanced sensitivity results from the suppression of oxide growth kinetics by the electropolished surface, which shifts anodization toward a regime in which pore morphology is governed more strongly by the competing effects of field-assisted oxide growth and dissolution. As a result, changes in anodization voltage and electrolyte temperature have a more pronounced influence on the resulting nanostructure.

3.3. Effect of Substrate Preparation on Film Adhesion

One of the practical properties of anodized Tantalum critical to the performance of protective and biocompatible coatings is anodic oxide film adhesion to the substrate. One of the previously identified limitations of current anodization methods for tantalum is the need for coatings capable of withstanding the minimum 30 N adhesion requirement for abrasion resistant applications [43,44]. Towards this goal, the presence of a fluoride or oxyfluoride rich barrier layer between the anodic oxide and the substrate is one of the drawbacks of fluorinated electrolytes due to the increased likelihood of film delamination [10,27–29]. A previous study of films grown in potassium phosphate-glycerol electrolyte reported the formation of a dense barrier layer over the course of 1-h anodization [31], and we observed formation of a similar layer in this study (Figure S1, Supplementary Information). Despite the presence of this barrier layer, films grown in potassium phosphate-glycerol electrolytes have previously been reported to display exceptional adhesion properties across multiple anodic metal oxides [45]. One possible mechanism for the improved adhesion of such films may be differences in the rate determining step for formation of the barrier layer between fluoride-containing and phosphate/glycerol electrolytes. Tsuji et al. investigated the relationship between barrier layer thickness and formation potential during formation of anodic TiO_2 in hot phosphate/glycerol electrolyte via cyclic voltammetry [46]. In fluoride-containing electrolyte, the electric field strength at the barrier layer was reported to decrease during the negative potential sweep, indicating a continuous increase in barrier layer thickness. In contrast, current density did not decrease even during the negative sweep in the hot phosphate/glycerol electrolyte, suggesting that diffusion of the oxygen sources in the electrolyte, rather than ion migration, may act as the rate determining step in barrier layer formation [46]. In the case of both their work on TiO_2 and our investigation of Ta_2O_5, the decrease in build up of foreign species at the interface may correspondingly promote direct contact between the anodic oxide and the metal substrate, improving oxide-substrate adhesion [28,47].

In order to investigate the influence of substrate pre-preparation and this type of barrier layer on the adhesion properties of the anodic oxide film, pull tests were performed in accordance with ASTM standard D4541-22 [48] on films grown at 20 V 180 °C on pristine, chemically etched, and electropolished substrates. The adhesion of anodic oxide layers grown on both chemically etched and electropolished samples showed significant improvement compared to oxide grown on the pristine substrate, resisting 96 MPa at a pull rate of 60 N/s even through repeated tests. Oxide removal was only achieved for the pristine sample following a 5 s hold under the same conditions, resulting in delamination of the oxide coating. No delamination or film rupture were observed for coatings grown on chemically etched and electropolished substrates, indicating a pull-off adhesion strength > 96 MPa. An inverse correlation was observed between the adhesion strength of the films and the oxide thickness measured by SEM (Figure 3). These results are in agreement with the higher strain resistance of thinner films previously reported by Choo and Devereux for films grown on chemically polished substrates, which was attributed to the ability of thin films to accommodate certain degrees of substrate slip not permitted in thicker films [49]. Further study would be necessary to determine the precise adhesion strength of the oxide films as well as deconvolute the effects of substrate roughness versus oxide thickness on film adhesion; however, the resistance of films grown on pre-prepared substrates to delamination under the tested conditions provides encouraging data with regard to the lower bounds of adhesion for coatings synthesized by this method. These results demonstrate the highly promising mechanical characteristics of films grown in potassium phosphate-based electrolyte as well as the potential benefits of substrate pre-preparation for such applications.

4. Conclusions

An effective strategy for improving the morphology and adhesion of anodic tantalum oxide films has been developed via electropolishing Ta foil substrates prior to anodization. Electropolishing reduced the substrate surface roughness below 6 nm while increasing the abundance of native suboxide species at the metal surface.

These surface modifications are hypothesized to alter the anodization kinetics by suppressing field-assisted oxide growth, thereby shifting the balance between anodic oxide growth and dissolution. As a result, films grown on electropolished substrates exhibited enhanced control over nanopore size and morphology as a function of anodization voltage, together with improved coating uniformity and stronger film–substrate adhesion. These results indicate that engineering the initial surface condition through electropolishing provides an effective route for tailoring anodic oxide growth. This approach offers a promising strategy for improving the fabrication of tantalum oxide coatings and may be extended to other anodic tantalum nanostructures, including highly ordered nanotubular architectures.

Supplementary Materials: The following supporting information can be downloaded at: https://media.sciltp.com/articles/others/2609031334329283/MI-26070174-SI.pdf. Figure S1: XPS O1s spectra for (a) pristine, (b) chemically etched, and (c) electropolished Ta foil.; Figure S2: Cross-sectional SEM of anodic tantalum oxide films grown at 20V180°C on (a) electropolished, (b) chemically etched, and (c) pristine substrates. Table S1: Quantitative oxidation-state fractions for XPS of pristine, chemically-etched, and electropolished samples.; Table S2: Pore sizes and wall thicknesses for films grown on chemically etched and electropolished substrates.

Author Contributions: H.X., S.E.P., C.K. and P.B. conceived and designed all experiments. S.E.P., C.K., M.B., T.M., G.C., S.F., K.K. and K.D. performed electropolishing and anodization. S.E.P. collected and analyzed SEM images. S.B.E. and J.A.R. performed AFM characterization. S.E.P. and S.B.E. performed XPS characterization, and S.E.P. and J.A.R. analyzed the data. J.O. performed adhesion testing utilizing equipment supplied by B.J. S.E.P. and H.X. drafted and revised the manuscript. All authors discussed the experimental results and coedited the manuscript.

Funding: This research was supported by the Department of Energy Office of Science, Basic Energy Sciences via award number DE-SC002648. S.P. acknowledges the support of the National Science Foundation (NSF) Graduate Research Fellowship Program (GRFP) (Grant No. 1946726) and the NSF Louis Stokes Alliance for Minority Participation (LSAMP) program, and gratefully acknowledges Dr. Elton Graugnard for use of the XPS in the Atomic Films Laboratory at Boise State University. T.M. and G.C. acknowledge support from ACS Project SEED. K.K. acknowledges support from NSF Award No. 1950305 (Boise State University, Materials for Society REU). This research utilized the AFM, XRD, and SEM instruments in the Boise State University FaCT Core Facility, RRID: SCR_024733, which receives support from the National Institutes of Health (NIH) under the Institutional Development Awards [IDeA] Program of the National Institute of General Medical Sciences (NIGMS) via Grants P20GM148321 and P20GM103408.

Institutional Review Board Statement: Not applicable.

Informed Consent Statement: Not applicable.

Data Availability Statement: The data that support the findings of this study are available from the corresponding authors on reasonable request.

Conflicts of Interest: The authors declare no conflict of interest.

Use of AI and AI-Assisted Technologies: No AI tools were utilized for this paper.

References

1. Momeni, M.M.; Mirhosseini, M.; Chavoshi, M.; Hakimizade, A. The Effect of Anodizing Voltage on Morphology and Photocatalytic Activity of Tantalum Oxide Nanostructure. *J. Mater. Sci. Mater. Electron.* **2016**, *27*, 3941–3947. https://doi.org/10.1007/s10854-015-4246-y.
2. Wang, W.; Yin, F.; Niu, H.; Li, Y.; Kim, E.S.; Kim, N.Y. Tantalum Pentoxide (Ta_2O_5 and Ta_2O_5-x)-Based Memristor for Photonic in-Memory Computing Application. *Nano Energy* **2023**, *106*, 108072. https://doi.org/10.1016/j.nanoen.2022.108072.
3. Li, J.; Jalbert, A.J.; Lee, S.; Simakas, L.S.; Geisler, N.J.; Watkins, V.J.; Cline, L.A.; Fuller, E.J.; Talin, A.A.; Li, Y. Nonvolatile Electrochemical Memory at 600 °C Enabled by Composition Phase Separation. *Device* **2025**, *3*, 100623. https://doi.org/10.1016/j.device.2024.100623.
4. Panda, D.; Hui, Y.-F.; Tseng, T.-Y. Diffusion Limiting Layer Induced Tantalum Oxide Based Memristor as Nociceptor. *Mater. Today Electron.* **2023**, *3*, 100031. https://doi.org/10.1016/j.mtelec.2023.100031.
5. Talin, A.A.; Li, Y.; Robinson, D.A.; Fuller, E.J.; Kumar, S. ECRAM Materials, Devices, Circuits and Architectures: A Perspective. *Adv. Mater.* **2023**, *35*, 2204771. https://doi.org/10.1002/adma.202204771.
6. Fialho, L.; Carvalho, S. Surface Engineering of Nanostructured Ta Surface with Incorporation of Osteoconductive Elements by Anodization. *Appl. Surf. Sci.* **2019**, *495*, 143573. https://doi.org/10.1016/j.apsusc.2019.143573.
7. Fialho, L.; Grenho, L.; Fernandes, M.H.; Carvalho, S. Porous Tantalum Oxide with Osteoconductive Elements and Antibacterial Core-Shell Nanoparticles: A New Generation of Materials for Dental Implants. *Mater. Sci. Eng. C* **2021**, *120*, 111761. https://doi.org/10.1016/j.msec.2020.111761.
8. Diamanti, M.V.; Pisoni, R.; Cologni, A.; Brenna, A.; Corinto, F.; Pedeferri, M. Anodic Oxidation as a Means to Produce Memristive Films. *J. Appl. Biomater. Funct. Mater.* **2016**, *14*, e290–e295. https://doi.org/10.5301/jabfm.5000290.

9. Dang, H.X.; Lin, Y.-M.; Klavetter, K.C.; Cell, T.H.; Heller, A.; Mullins, C.B. Lithium Insertion/Deinsertion Characteristics of Nanostructured Amorphous Tantalum Oxide Thin Films. *ChemElectroChem* **2014**, *1*, 158–164. https://doi.org/10.1002/celc.201300139.
10. Gonçalves, R.V.; Migowski, P.; Wender, H.; Eberhardt, D.; Weibel, D.E.; Sonaglio, F.C.; Zapata, M.J.M.; Dupont, J.; Feil, A.F.; Teixeira, S.R. Ta_2O_5 Nanotubes Obtained by Anodization: Effect of Thermal Treatment on the Photocatalytic Activity for Hydrogen Production. *J. Phys. Chem. C* **2012**, *116*, 14022–14030. https://doi.org/10.1021/jp303273q.
11. Su, Z.; Grigorescu, S.; Wang, L.; Lee, K.; Schmuki, P. Fast Fabrication of Ta_2O_5 Nanotube Arrays and Their Conversion to Ta3N5 for Efficient Solar Driven Water Splitting. *Electrochem. Commun.* **2015**, *50*, 15–19. https://doi.org/10.1016/j.elecom.2014.10.017.
12. Han, C.; Wang, T. Tantalum Pentoxide: From Crystal Structures to Applications in Water Splitting. *Energy Fuels* **2023**, *37*, 13624–13644. https://doi.org/10.1021/acs.energyfuels.3c02295.
13. Melody, B. The Non-Thickness-Limited Growth of Anodic Oxide Films on Valve Metals. *Electrochem. Solid-State Lett.* **1999**, *1*, 126. https://doi.org/10.1149/1.1390659.
14. Zhou, X.; Nguyen, N.T.; Özkan, S.; Schmuki, P. Anodic TiO_2 Nanotube Layers: Why Does Self-Organized Growth Occur—A Mini Review. *Electrochem. Commun.* **2014**, *46*, 157–162. https://doi.org/10.1016/j.elecom.2014.06.021.
15. Piotrowski, O.; Madore, C.; Landolt, D. Electropolishing of Tantalum in Sulfuric Acid–Methanol Electrolytes. *Electrochimica Acta* **1999**, *44*, 3389–3399. https://doi.org/10.1016/S0013-4686(99)00056-0.
16. Barnes, P.; Savva, A.; Dixon, K.; Bull, H.; Rill, L.; Karsann, D.; Croft, S.; Schimpf, J.; Xiong, H. Electropolishing Valve Metals with a Sulfuric Acid-Methanol Electrolyte at Low Temperature. *Surf. Coat. Technol.* **2018**, *347*, 150–156. https://doi.org/10.1016/j.surfcoat.2018.04.082.
17. Wu, M.T.; Leu, I.C.; Hon, M.H. Effect of Polishing Pretreatment on the Fabrication of Ordered Nanopore Arrays on Aluminum Foils by Anodization. *J. Vac. Sci. Technol. B Microelectron. Nanometer Struct. Process. Meas. Phenom.* **2002**, *20*, 776–782. https://doi.org/10.1116/1.1467657.
18. Rauf, A.; Mehmood, M.; Asim Rasheed, M.; Aslam, M. The Effects of Electropolishing on the Nanochannel Ordering of the Porous Anodic Alumina Prepared in Oxalic Acid. *J. Solid State Electrochem.* **2009**, *13*, 321–332. https://doi.org/10.1007/s10008-008-0550-2.
19. Lee, B.G.; Hong, S.-Y.; Yoo, J.E.; Choi, J. Electropolishing for the Formation of Anodic Nanotubular TiO2 with Uniform Length and Density. *Appl. Surf. Sci.* **2011**, *257*, 7190–7194. https://doi.org/10.1016/j.apsusc.2011.03.089.
20. Fialho, L.; Almeida Alves, C.F.; Marques, L.S.; Carvalho, S. Development of Stacked Porous Tantalum Oxide Layers by Anodization. *Appl. Surf. Sci.* **2020**, *511*, 145542. https://doi.org/10.1016/j.apsusc.2020.145542.
21. Singh, S.; Barden, W.R.T.; Kruse, P. Nanopatterning of Transition Metal Surfaces via Electrochemical Dimple Array Formation. *ACS Nano* **2008**, *2*, 2453–2464. https://doi.org/10.1021/nn8003789.
22. Shimizu, K.; Kobayashi, K.; Thompson, G.E.; Skeldon, P.; Wood, G.C. Anodic Oxide Films on Tantalum: Incorporation and Mobilities of Electrolyte-Derived Species. *Philos. Mag. B* **1996**, *73*, 461–485. https://doi.org/10.1080/13642819608239129.
23. Mohapatra, B.D.; Sulka, G.D. Review of Anodic Tantalum Oxide Nanostructures: From Morphological Design to Emerging Applications. *ACS Appl. Nano Mater.* **2024**, *7*, 13865–13892. https://doi.org/10.1021/acsanm.4c02000.
24. Ngadiman, N.L.S.; Abdul Rani, R.; Makhsin, S.R.; Ayub, M.A.; Aryani, D.; Zoolfakar, A.S. Properties and Application of Electrochemically Anodized Ta_2O_5 Nanostructures: A Review. *J. Mech. Eng.* **2022**, *11*, 1–48. https://doi.org/10.24191/jmeche.v11i1.23580.
25. Horwood, C.A.; El-Sayed, H.A.; Birss, V.I. Precise Electrochemical Prediction of Short Tantalum Oxide Nanotube Length. *Electrochimica Acta* **2014**, *132*, 91–97. https://doi.org/10.1016/j.electacta.2014.03.128.
26. Barton, J.E.; Stender, C.L.; Li, P.; Odom, T.W. Structural Control of Anodized Tantalum Oxide Nanotubes. *J. Mater. Chem.* **2009**, *19*, 4896–4898. https://doi.org/10.1039/B904964A.
27. El-Sayed, H.A.; Birss, V.I. Controlled Interconversion of Nanoarray of Ta Dimples and High Aspect Ratio Ta Oxide Nanotubes. *Nano Lett.* **2009**, *9*, 1350–1355. https://doi.org/10.1021/nl803010v.
28. Singh, S.; Festin, M.; Barden, W.R.T.; Xi, L.; Francis, J.T.; Kruse, P. Universal Method for the Fabrication of Detachable Ultrathin Films of Several Transition Metal Oxides. *ACS Nano* **2008**, *2*, 2363–2373
29. Gonçalves, R.V.; Wojcieszak, R.; Uberman, P.M.; Teixeira, S.R.; Rossi, L.M. Insights into the Active Surface Species Formed on Ta_2O_5 Nanotubes in the Catalytic Oxidation of CO. *Phys. Chem. Chem. Phys.* **2014**, *16*, 5755. https://doi.org/10.1039/c3cp54887b.
30. Almeida Alves, C.F.; Calderon, V.S.; Ferreira, P.J.; Marques, L.; Carvalho, S. Passivation and Dissolution Mechanisms in Ordered Anodic Tantalum Oxide Nanostructures. *Appl. Surf. Sci.* **2020**, *513*, 145575. https://doi.org/10.1016/j.apsusc.2020.145575.
31. Lee, K.; Schmuki, P. Highly Ordered Nanoporous Ta_2O_5 Formed by Anodization of Ta at High Temperatures in a Glycerol/Phosphate Electrolyte. *Electrochem. Commun.* **2011**, *13*, 542–545. https://doi.org/10.1016/j.elecom.2011.03.005.

32. Uslu, E.; Mimiroglu, D.; Ercan, B. Nanofeature Size and Morphology of Tantalum Oxide Surfaces Control Osteoblast Functions. *ACS Appl. Bio Mater.* **2021**, *4*, 780–794. https://doi.org/10.1021/acsabm.0c01354.
33. Sanz, J.M.; Hofmann, S. Auger Electron Spectroscopy and X-Ray Photoelectron Spectroscopy Studies of the Oxidation of Polycrystalline Tantalum and Niobium at Room Temperature and Low Oxygen Pressures. *J. Common Met.* **1983**, *92*, 317–327. https://doi.org/10.1016/0022-5088(83)90498-8.
34. *NIST X-ray Photoelectron Spectroscopy Database*, Version 5.0; NIST X-ray Photoelectron Spectroscopy Database (SRD 20); NIST: Washington, DC, USA, 2023. https://doi.org/10.18434/T4T88K.
35. Chakraborti, P.; Sharma, H.; Pulugurtha, M.R.; Gandhi, S.; Tummala, R.R. Oxide Composition Studies of Electrochemically Grown Tantalum Oxide on Sintered Tantalum Using XPS Depth-Profiling and Co-Relation with Leakage Properties. *J. Mater. Sci. Mater. Electron.* **2017**, *28*, 18773–18780. https://doi.org/10.1007/s10854-017-7826-1.
36. Khanuja, M.; Sharma, H.; Mehta, B.R.; Shivaprasad, S.M. XPS Depth-Profile of the Suboxide Distribution at the Native Oxide/Ta Interface. *J. Electron Spectrosc. Relat. Phenom.* **2009**, *169*, 41–45. https://doi.org/10.1016/j.elspec.2008.10.004.
37. Díaz, B.; Światowska, J.; Maurice, V.; Seyeux, A.; Härkönen, E.; Ritala, M.; Tervakangas, S.; Kolehmainen, J.; Marcus, P. Tantalum Oxide Nanocoatings Prepared by Atomic Layer and Filtered Cathodic Arc Deposition for Corrosion Protection of Steel: Comparative Surface and Electrochemical Analysis. *Electrochimica Acta* **2013**, *90*, 232–245. https://doi.org/10.1016/j.electacta.2012.12.007.
38. Macak, J.M.; Tsuchiya, H.; Ghicov, A.; Yasuda, K.; Hahn, R.; Bauer, S.; Schmuki, P. TiO_2 Nanotubes: Self-Organized Electrochemical Formation, Properties and Applications. *Curr. Opin. Solid State Mater. Sci.* **2007**, *11*, 3–18. https://doi.org/10.1016/j.cossms.2007.08.004.
39. Mor, G.K.; Varghese, O.K.; Paulose, M.; Shankar, K.; Grimes, C.A. A Review on Highly Ordered, Vertically Oriented TiO_2 Nanotube Arrays: Fabrication, Material Properties, and Solar Energy Applications. *Sol. Energy Mater. Sol. Cells* **2006**, *90*, 2011–2075. https://doi.org/10.1016/j.solmat.2006.04.007.
40. Ma, J.-W.; Zan, R.; Chen, W.-Z.; Ni, J.-H.; Zhang, X.-N. Cell Behaviors on Surface of Pure Tantalum with Nano-Dimpled Structure. *Rare Met.* **2019**, *38*, 543–551. https://doi.org/10.1007/s12598-019-01226-1.
41. Schmuki, P. Self-Organized Oxide Nanotube Layers on Titanium and Other Transition Metals. In *Electrochemistry at the Nanoscale*; Schmuki, P., Virtanen, S., Eds.; Springer: New York, NY, 2009; pp 435–466. https://doi.org/10.1007/978-0-387-73582-5_12.
42. El-Sayed, H.A.; Molero, H.M.; Birss, V.I. The Impact of Fabrication Conditions on the Quality of Au Nanoparticle Arrays on Dimpled Ta Templates. *Nanotechnology* **2012**, *23*, 435602. https://doi.org/10.1088/0957-4484/23/43/435602.
43. Ding, Z.; Tang, Y.; Liu, L.; Ding, Z.; Tan, Y.; He, Q. Improving the Adhesive, Mechanical, Tribological Properties and Corrosion Resistance of Reactive Sputtered Tantalum Oxide Coating on Ti6Al4V Alloy via Introducing Multiple Interlayers. *Ceram. Int.* **2022**, *48*, 5983–5994. https://doi.org/10.1016/j.ceramint.2021.11.134.
44. Hogmark, S.; Jacobson, S.; Larsson, M. Design and Evaluation of Tribological Coatings. *Wear* **2000**, *246*, 20–33. https://doi.org/10.1016/S0043-1648(00)00505-6.
45. Li, P.; Li, C.; Zhang, Z.; Zhu, X.; Song, Y. Anodic Oxide Films Grown in Dehydrated Phosphate/Glycerol Electrolytes at High Temperatures. *Langmuir* **2024**, *40*, 25758–25771. https://doi.org/10.1021/acs.langmuir.4c03777.
46. Tsuji, E.; Matsuura, S.; Aoki, Y.; Habazaki, H. Diffusion-Controlled Growth of TiO_2 Mesoporous Anodic Films in Hot Phosphate/Glycerol Electrolytes. *Electrochemistry* **2018**, *86*, 184–189. https://doi.org/10.5796/electrochemistry.18-00005.
47. Singh, S.; Greiner, M.T.; Kruse, P. Robust Inorganic Membranes from Detachable Ultrathin Tantalum Oxide Films. *Nano Lett.* **2007**, *7*, 2676–2683. https://doi.org/10.1021/nl071061z.
48. *ASTM D4541-22*; Standard Test Method for Pull-Off Strength of Coatings Using Portable Adhesion Testers. ASTM: West Conshohocken, PA, USA, 2026.
49. Choo, Y.H.; Devereux, O.F. Mechanical Failure of Anodic Films on Aluminum and Tantalum. *J. Electrochem. Soc.* **1976**, *123*, 1868. https://doi.org/10.1149/1.2132714.